ORIGINAL COMMUNICATION

Three-Dimensional Study of the Musculotendinous Architecture of Lumbar Multifidus and Its Functional Implications

ALESSANDRO L. ROSATELLI,* **KAJEANDRA RAVICHANDIRAN,** AND **ANNE M. AGUR**

Department of Surgery, Division of Anatomy, University of Toronto, Toronto, Canada

Lumbar multifidus (LMT) is a key muscle, which provides stability to the lumbar spine, and has been shown to have altered neuromuscular recruitment following acute episodes of low back pain. Architectural parameters are important determinants of function, but have not been well documented for LMT. Therefore, the purpose of this study is to model and quantify the architecture of LMT throughout its volume. Nine male and one female formalin-embalmed cadaveric specimens (average age 80 ± 11 years) without any evidence of spinal deformity/pathology were used. The musculotendinous components of LMT were serially dissected and digitized. Next, the data were imported into MAYA^{TM} to create a three-dimensional model of each segment of LMT from which architectural parameters including fiber bundle length (FBL), fiber bundle angle (FBA), and tendon length were quantified. Water displacement was used to determine volume. The data were analyzed using paired t-tests and ANOVA followed by Tukey's post-hoc test ($P \leq 0.05$). LMT (L1–L4) has three architecturally distinct regions: superficial, intermediate, and deep. Intermediate LMT was absent in all specimens at L5. Mean FBL decreased significantly ($P \leq 0.05$) from superficial (5.8 ± 1.6 cm) to deep (2.9 ± 1.1 cm) as did volume (superficial, 5.6 ± 2.3 ml; deep, 0.7 ± 0.3 ml) measured at each region. By contrast, mean FBA increased from superficial to deep. The current study lends further evidence to support the role of different regions within LMT to serve distinct functions particularly to produce movement and/or control stability. Clin. Anat. 21:539–546, 2008. © 2008 Wiley-Liss, Inc.

Key words: back muscles; cadavers; computer modeling; 3D; tendon; angle; length; volume

INTRODUCTION

Lumbar multifidus (LMT) is structurally and architecturally complex, being the most medial and largest back muscle spanning the lumbosacral junction (Macintosh et al., 1986). The importance of this muscle in spinal stability is well documented (Donisch and Basmajian, 1972; Cholewicki et al., 1997; Solomonow et al., 1998; Moseley et al., 2002) and there is clinical and ultrasonographic evidence, which demonstrates that LMT becomes inhibited in patients with acute low back pain (Hides et al., 1996). Alteration in the neuromuscular recruitment of this muscle following an episode of back pain is postulated to predispose the lumbar spine to further injury and instability (Hides et al., 2001). To understand how the back muscles and in particular LMT controls spinal stability, investigators commonly use biomechanical models. Despite their complexity, LMT

TABLE 1. Architectural Data From Previous Studies

Level	Ant-Post Angle (°) [Macintosh et al., 1986]	Muscle Fiber Angulation (°) [De Foa et al., 1989]	Muscle Fiber Angulation (°) [Biedermann et al., 1991]	Fascicle Length (cm) [Bogduk et al., 1992]
L1-L4	14.8 ± 0.8	Male 15.1 ± 1.43	Female 23.5 ± 4.5	11.1
L1-L5	15.0 ± 0.7	$(13.5–18.0 \pm 1.0)$	$(17.5–28.5)$	14.6
L1-S1	12.6 ± 0.6			17.7
L1-Sacrum	16.6 ± 0.9			19.0
L2-L5	18.8 ± 1.1			9.8
L2-S1	18.0 ± 1.0			12.4
L2-Sacrum	20.0 ± 1.6			15.4
L3-S1	23.2 ± 1.1			8.0
L3-Sacrum	19.6 ± 0.9			11.9
L4-Sacrum	15.6 ± 0.9			7.3
L5-Sacrum	5.4 ± 1.5			4.1

and the other back muscles are commonly incorporated into these models in an "abridged manner, reducing their actions more or less to a single force equivalent" (Hansen et al., 2006). A great deal of architectural data is lost in the process, data which is inherently important in determining the nature, distribution and types of forces acting through the lumbar spine. The architectural data which is lost includes measurements of fiber bundle angle (FBA), fiber bundle length (FBL), and muscle volume. Hence, the ability to extrapolate the actions of the back muscles from these models is dependant on the accuracy of the architectural data used as input parameters (Hansen et al., 2006).

Previous studies of LMT have been primarily descriptive with few quantitative studies investigating architectural parameters such as FBA, FBL, and volume (Macintosh and Bogduk, 1986; De Foa et al., 1989; Biedermann et al., 1991; Bogduk et al.,1992). Macintosh and Bogduk (1986) studied the orientation of the fascicles of the LMT in five cadaveric specimens and summarized the descriptive data by plotting the orientation of a total of eleven fascicles with respect to its vertebrae of origin. These authors then measured the angle of each fascicle with respect to a standard reference line through each vertebra in both antero-posterior and lateral radiographs of the lumbar spine. The lengths of these fascicles were reported in a subsequent article as the "projected length of each fascicle as viewed in lateral radiographs" (Bogduk et al., 1992). Bogduk et al. (1992) state that muscle volume had been measured using water displacement in a previous study (Macintosh and Bogduk, 1986) but did not report the volumetric data. De Foa et al. (1989) using photographs of four male cadaveric specimens and in a follow up study by Biedermann et al. (1991) using six female cadaveric specimens reported "muscle fiber direction" relative to anatomical reference lines and the spine. The results of these studies are summarized in Table 1. Although these studies provide reference data on some architectural parameters important in defining muscle function, lacking are studies which quantify the musculotendinous architecture of LMT throughout its volume. Recent advances in the study of skeletal muscle architecture which combines anatomical microdissection techniques with new computer graphics and digitization software has allowed skeletal muscle architecture to be visualized and quantified accurately (Ng-Thow-Hing, 2001; Agur et al., 2003). Therefore, the purpose of this study is to quantify the muscle architecture of the human LMT throughout its volume. An accurate three dimensional model of LMT could then be constructed and used to clarify its functional characteristics.

MATERIALS AND METHODS

Specimens

Ten formalin embalmed human cadaveric specimens (9 M/1 F) with a mean age of 80 ± 11 years were studied. Specimens with visible evidence of musculoskeletal deformity, muscle pathology, indication of previous surgery or trauma were excluded. Ethics approval was received from the Chief Coroner and General Inspector of Anatomy of the Province of Ontario and from the University of Toronto.

Dissection, Digitization, and Three-Dimensional Modeling

The LMT was exposed unilaterally by removing the skin, fascia, superficial muscles, and aponeuroses. Each specimen was securely bound to a metal tray and three reference points (bilateral posterior superior iliac spines, and sacral apex) were demarcated clearly using screws. These reference points were necessary in order to ensure the accuracy and consistency of the digitized data collected. Using a $1.75\times$ magnifier, muscle fiber bundles of LMT were identified and traced along their full length craniocaudally starting at the L1 spinous process. The course of each fiber bundle was delineated by marking its proximal and distal attachment sites and 5–20 intervening points using a fine paint pen. The x, y, and z coordinates of each point were then obtained using a Microscribe® G2 Digitizer (Immersion Corporation, San Jose, CA). The removal of individual fiber bundles permitted the identification, marking, and digitization of successively deeper segments of the muscle. The dissection and digitization process continued sequentially from cranial to caudal
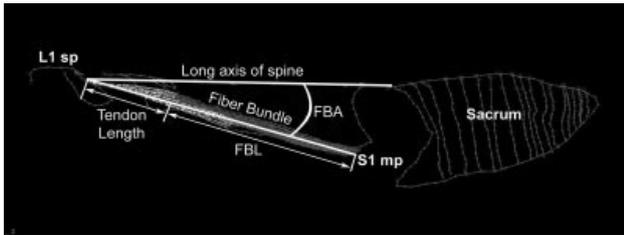
Fig. 1. Calculation of muscle fiber bundle length (FBL) and fiber bundle angle (FBA). Spinous process (sp); mammillary process (mp).

and from superficial to deep until the entire LMT had been resected from the lumbar spine, ilium, and sacrum. In addition, during serial dissection the entire surface of each tendon was marked with 20–80 curves and then digitized. Additionally, the periphery of the spinous process and lamina of each lumbar vertebra, the sacrum, and ilium were similarly captured.

The digitized data were used to reconstruct the structure of the LMT as it appeared in situ using Alias® MAYA™ (a specialized software used in three-dimensional modeling and animation), which was customized with software developed in our laboratory. The virtual model created for each specimen was then used to visualize and document the morphology of LMT (i.e., attachment sites, spatial orientation, distribution of fiber bundles, and associated tendons in relation to bony structures) throughout its volume. Morphological differences observed within the LMT were used to identify architecturally distinct regions.

Architectural Parameters and Data Analysis

The architectural parameters of LMT investigated in this study were FBL, FBA, extramuscular tendon length and volume. FBL (cm) was calculated as the sum of the distances between each of the digitized points along the length of the fiber bundle. FBA (degrees) was defined as the angle formed in the sagittal plane between a tangent line drawn through the centre of each lumbar spinous process (L1-L5) and the fiber bundles attaching to these vertebrae. Extramuscular tendon length (cm) was computed as the average length of all digitized curves spanning between the superior and inferior ends of the tendon (Fig. 1). Volume (ml) was determined using water displacement (Bogduk et al., 1992).

Tendon length, FBL and FBA were calculated using computer algorithms. The architectural parameters were then characterized with descriptive statistics (mean and standard deviation). Paired t-test and ANOVA followed by Tukey's post-hoc were carried out to compare means ($P < 0.05$).

RESULTS

The unique modeling technique used in this study allowed both visualization and quantification of musculotendinous morphology and architecture. The LMT

was found to consist of five bands in all 10 specimens, each originating from a lumbar spinous process/lamina (L1–L5). Muscle fiber bundles within each band having similar medial and lateral points of attachment were used to identify architecturally distinct regions. The L1–L4 bands were found to consist of three regions: superficial, intermediate, and deep, while the L5 band had only two regions: superficial and deep (Figs. 2A, 2G, and 2J).

Superficial LMT

The fiber bundles of superficial LMT attached proximally via a common tendon to the tips of the spinous processes (L1–L5) and passed inferolaterally to the mammillary processes of L5, S1, sacrum and ilium. The portion of superficial LMT originating from:

- L1 spinous process had three segments attaching distally to the L5 and S1 mammillary process and posterior superior iliac spine (PSIS) respectively (Fig. 2B).
- L2 spinous process had two segments, attaching distally to the S1 mammillary process and PSIS respectively (Fig. 2C).
- L3 spinous process had one segment which attached distally to the dorsolateral aspect of the sacrum between the first to third sacral segments (Fig. 2D).
- L4 spinous process consisted of one segment which attached to the posterior surface of the sacrum between the second to fourth sacral segments, medial to the distal attachment of L3 (Fig. 2E).
- L5 spinous process had one segment which attached to the posterior surface of the sacrum between the level of the third to fourth sacral segments, lateral to the median crest of the sacrum but medial to the distal attachment of L4 (Fig. 2F).

Intermediate LMT

Intermediate LMT had a muscular proximal attachment to the spinous processes of L1–L4. Distally, L1, L2, and L3 portions attached via tendons to the L4, L5, and S1 mammillary processes, respectively. However, the L4 portion attached onto the sacrum at the S2 level (Fig. 2H). The intermediate LMT was absent at L5 in all specimens (Fig. 2J).

Deep LMT

Deep LMT consisted of five segments (L1–L5) which where entirely muscular. Each segment attached superiorly to the lamina of lumbar vertebra L1–L5, and inferiorly two levels below to the L3, L4, L5, and S1 mammillary process, respectively, while the L5 fascicle attached to the sacrum (Fig. 2I). Segmental fatty replacement was observed in three specimens.

Architectural Parameters

Mean FBL was significantly different between the three regions ($P \leq 0.05$). Deep LMT had the shortest
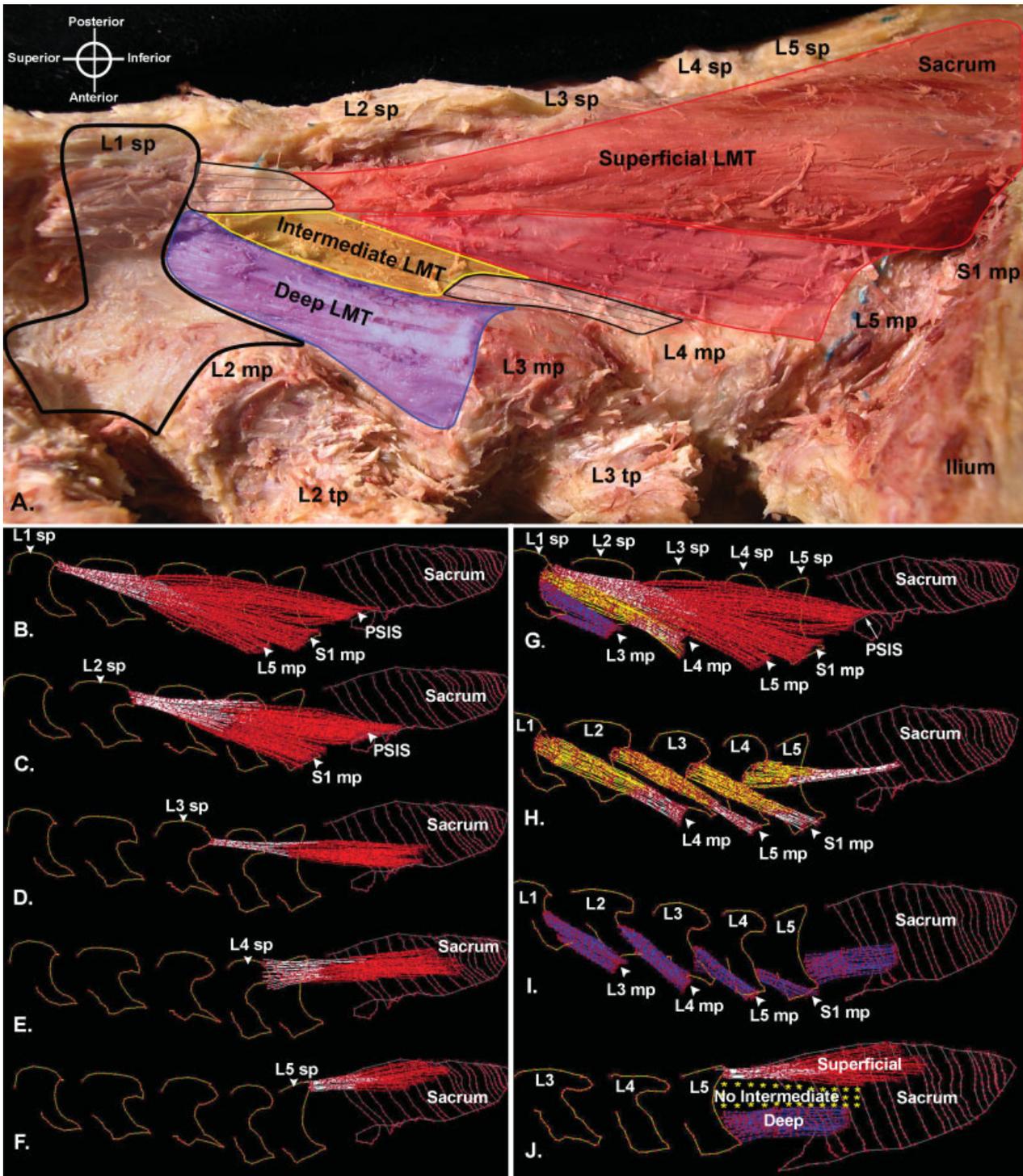
Fig. 2. Dissection, digitization, and three-dimensional modeling of lumbar multifidus, lateral views. **A**: Dissection of superficial (red), intermediate (yellow), and deep (purple) regions. **B, C, D, E, F**: Segments of the superficial region attaching to L1–L5 spinous processes. **G**: Three-dimensional reconstruction of the digitized specimen shown in A. **H**: Segments of the intermediate region attaching to the L1–L4 spinous processes. Note that there is no intermediate LMT attaching to the spinous process at L5. **I**: Segments of the deep region attaching to the L1–L5 laminae. **J**: Regions of LMT attaching to the L5 spinous process. Intermediate LMT is absent at L5. LMT, lumbar multifidus; sp, spinous process; mp, mammillary process; tp, transverse process; PSIS, posterior superior iliac spine; L, lumbar.

TABLE 2. Summary of Mean FBL of LMT

LMT		Mean FBL (cm)		
	Segment(s)	Level	Region
Superficial				
L1	to L5	6.0 ± 1.8	7.3 ± 1.7[a]	
	to S1	6.9 ± 1.7		
	to PSIS	8.4 ± 2.0		
L2	to S1	5.5 ± 1.5	6.4 ± 1.0[a,b]	5.8 ± 1.6[a]
	to PSIS	6.8 ± 1.2		
L3	to Sa	*	5.6 ± 1.1[b,c]	
L4	to Sa	*	4.8 ± 1.2[c]	
L5	to Sa	*	4.8 ± 1.7[c]	
Intermediate				
L1	to L4	*	3.9 ± 1.7[d]	
L2	to L5	*	4.4 ± 1.8[d]	4.1 ± 1.5[b]
L3	to S1	*	3.9 ± 1.6[d]	
L4	to Sa	*	4.1 ± 0.9[d]	
L5	–	X	X	
Deep				
L1	to L3	*	2.6 ± 0.6[e]	
L2	to L4	*	2.7 ± 0.8[e]	
L3	to L5	*	2.6 ± 0.8[e]	2.9 ± 1.1[c]
L4	to S1	*	3.0 ± 1.3[e]	
L5	to Sa	*	3.6 ± 1.4[e]	

The superscript letters are used to indicate the presence or absence of statistical significance (analysis of variance) between the three regions or among levels within a region. If the superscripts in a column differ, then the result is statistically significant. If the letter is repeated, there is no statistical significance. PSIS, posterior superior iliac spine; Sa, sacrum; FBL, mean fiber bundle length; X, absent at this level.

*, only one segment present at these levels, hence mean FBL for segment equals mean FBL for level.

mean FBL (2.9 ± 1.1 cm) while superficial had the longest (5.8 ±1.6 cm). Intermediate LMT had a mean FBL of 4.1 ± 1.5 cm. Comparison of FBL among levels L1 through L5 within a given region was shown to be significant for the superficial region only. Fiber bundles attaching proximally to the L1 and L2 spinous processes had the longest FBL, while those attaching to the L4 and L5 spinous processes had the shortest (Table 2).

In contrast to FBL, changes in mean FBA were not significant ($P = 0.0869$), but increased from the superficial to deep regions of LMT (Table 3). The largest angle was found in the deep region at the L5 level (28.0 ± 11.8°). The average FBA calculated within levels of the superficial and intermediate regions and the L1–L4 levels of the deep region were similar ranging from 11.7° to 17.2°.

Average volumes for the superficial, intermediate, and deep region were significantly different from one another and decreased from superficial to deep (Table 4). Within the superficial region, the mean volume of the L1 to L3 levels was significantly larger than the L4 and L5 levels. In the deep region, the L5 level had a significantly larger volume compared with the L1 to L4 levels. No significant difference in mean volumes was noted within the levels of the intermediate region.

Tendon Architecture

The superficial and intermediate regions of LMT were both found to have extramuscular tendons associated with their bony attachments, whereas the deep region was entirely muscular. The L1–L5 segments of the superficial region each have a common tendon attaching medially to the corresponding spinous process (Fig. 2B–F). In contrast the tendon of the intermediate region was located laterally attaching the fiber bundles to the mammillary processes of L4, L5, S1 and the sacrum (Fig. 2H). The tendons of the superficial region were thick and cylindrical, whereas the tendons of the intermediate region were thin and flat. Although the shape of the tendinous components of the superficial and intermediate regions differed, the average tendon lengths were similar, 2.4 ± 0.1 cm and 2.3 ± 0.6 cm, respectively (Table 5).

DISCUSSION

Using micro-dissection and three dimensional modeling techniques we were able to capture the architecture of LMT throughout its volume by digitizing up to 1,400 individual muscle fiber bundles per specimen. This method, unlike previous studies which simplify the morphology and architecture of

TABLE 3. Summary of Mean FBA of LMT

LMT		Mean FBA (°)		
	Segment(s)	Level	Region
Superficial				
L1	to L5	14.3 ± 8.0	14.5 ± 7.7[a]	
	to S1	12.4 ± 8.9		
	to PSIS	16.4 ± 11.8		
L2	to S1	12.5 ± 3.9	14.4 ± 5.1[a]	13.7 ± 6.9[a]
	to PSIS	16.0 ± 6.2		
L3	to Sa	*	11.7 ± 5.4[a]	
L4	to Sa	*	12.6 ± 8.0[a]	
L5	to Sa	*	15.3 ± 8.4[a]	
Intermediate				
L1	to L4	*	15.9 ± 6.7[a]	
L2	to L5	*	14.0 ± 3.9[a]	
L3	to S1	*	16.4 ± 8.9[a]	15.3 ± 7.0[a]
L4	to Sa	*	14.8 ± 8.6[a]	
L5	–	X	X	
Deep				
L1	to L3	*	13.1 ± 5.0[a]	
L2	to L4	*	15.9 ± 5.6[a,b]	
L3	to L5	*	17.2 ± 12.1[a,b]	18.3 ± 10.4[a]
L4	to S1	*	16.7 ± 10.1[a,b]	
L5	to Sa	*	28.0 ± 11.8[b]	

The superscript letters are used to indicate the presence or absence of statistical significance (analysis of variance) between the three regions or among levels within a region. If the superscripts in a column differ, then the result is statistically significant. If the letter is repeated, there is no statistical significance. PSIS, posterior superior iliac spine; Sa, sacrum; FBA, mean fiber bundle angle; X, absent at this level.

*, only one segment present at these levels, hence mean FBA for segment equals mean FBA for level.

TABLE 4. Summary of Mean Volume of LMT

LMT		Segment(s)	Mean Volume (ml) Level	Region
Superficial				
L1	to L5	1.1 ± 0.2	6.7 ± 0.5[a]	
	to S1	1.6 ± 0.6		
	to PSIS	3.9 ± 0.7		
L2	to S1	1.6 ± 0.4	7.9 ± 1.9[a]	5.6 ± 2.3[a]
	to PSIS	6.3 ± 1.6		
L3	to Sa	*	7.0 ± 1.7[a]	
L4	to Sa	*	3.7 ± 0.4[b]	
L5	to Sa	*	2.8 ± 0.3[b]	
Intermediate				
L1	to L4	*	1.7 ± 0.4[a]	
L2	to L5	*	1.9 ± 0.3[a]	1.7 ± 0.4[b]
L3	to S1	*	1.5 ± 0.3[a]	
L4	to Sa	*	1.8 ± 0.5[a]	
L5	–	X	X	
Deep				
L1	to L3	*	0.5 ± 0.1[a]	
L2	to L4	*	0.6 ± 0.2[a]	
L3	to L5	*	0.6 ± 0.2[a]	0.7 ± 0.3[c]
L4	to S1	*	0.5 ± 0.1[a]	
L5	to Sa	*	1.3 ± 0.1[b]	

The superscript letters are used to indicate the presence or absence of statistical significance (analysis of variance) between the three regions or among levels within a region. If the superscripts in a column differ, then the result is statistically significant. If the letter is repeated, there is no statistical significance. PSIS, posterior superior iliac spine; Sa, sacrum; X, absent at this level.
*, only one segment present at these levels, hence mean volume for segment equals mean volume for level.

LMT using straight lines to represent the muscle and its line of action (Macintosh and Bogduk, 1986; Macintosh et al., 1986) allows individual muscle fiber bundles to be visualized in three-dimensions and their architectural characteristics (i.e. FBL and FBA) to be quantified. The three dimensional reconstruction of the muscle enables viewing and quantification of the architecture at a level of complexity which could not be achieved previously (Agur et al., 2003; Kim et al., 2007).

Morphology and Muscle Architecture

Muscle morphology, in particular, architectural parameters such as FBA and FBL are important determinants of function, and can have significant effects on a muscle's force generating capability (Roy and Ishihara, 1997; Lieber and Friden, 2000). In addition, the orientation of fiber bundles within a muscle may be used to determine its actions (Macintosh and Bogduk, 1986) and is integral to ensuring imaging guided electrode placement with electromyography power spectrum assessment (De Foa et al., 1989; Biedermann et al., 1991).

Few studies have documented the morphology of LMT with "anatomical texts and atlases describing muscle structure mainly in terms of their origins and insertions" (Biedermann et al., 1991). In a cadaveric study ($n = 12$), Macintosh et al. (1986) found LMT to consist of five bands (L1–L5), with each band originating from a lumbar spinous process and inserting distally onto mammillary process(es), the sacrum and/or the ilium. In the current study, LMT was also found to consist of five bands; however, individual fiber bundles making up each band can be further divided into distinct regions using morphological characteristics including FBL, FBA, muscle length, volume, placement of tendinous components and attachment sites. The L1 to L4 bands could be subdivided into three regions: superficial, intermediate, and deep. However, the L5 band consisted of only two regions: superficial and deep. At L5, the intermediate region was absent in all 10 specimens.

The current study quantified key architectural parameters for the three regions of LMT. Regional differences in FBA, FBL, and volume have important functional implications. Based on the results of this study, superficial LMT seems well suited to generate posterior sagittal rotation (lumbar extension) as it has:

- the most numerous and longest fiber bundles;
- the largest volume;
- several points of attachment laterally onto the mammillary processes and sacrum/ilium;
- muscle fiber bundles with smaller FBA (that is, muscle fibers more vertically oriented relative to the sagittal plane).

While Macintosh and Bogduk (1986) also suggested that the "principal action of multifidus is posterior sagittal rotation," the current study found the FBA of superficial LMT at L5 to be 10° greater than that reported previously by these authors (Table 1 and Table 3). The relatively large FBA at L5 suggests that LMT at this level is also important in controlling rotational movement in the transverse plane at the lumbosacral junction.

Although the action of a muscle may be determined from the orientation of its muscle fibers (Mac-

TABLE 5. Summary of Mean Tendon Length and Muscle Length of LMT

Region	Mean TL (cm)	Mean FBL (cm)	TL + FBL* (cm)
Superficial	2.4 ± 0.1	5.8 ± 1.6	8.2 ± 1.6
L1	2.7 ± 0.8	7.3 ± 1.7	10.0 ± 1.9
L2	2.4 ± 0.9	6.4 ± 1.0	8.8 ± 1.4
L3	2.4 ± 0.8	5.6 ± 1.1	7.9 ± 1.4
L4	2.4 ± 0.8	4.8 ± 1.2	7.2 ± 1.4
L5	2.4 ± 0.7	4.8 ± 1.7	7.2 ± 1.8
Intermediate	2.3 ± 0.6	4.1 ± 1.5	6.4 ± 1.6
L1	2.0 ± 0.9	3.9 ± 1.7	5.9 ± 1.9
L2	2.1 ± 0.6	4.4 ± 1.8	6.5 ± 1.9
L3	2.0 ± 0.7	3.9 ± 1.6	5.9 ± 1.8
L4	3.3 ± 0.9	4.1 ± 0.9	7.3 ± 1.3
L5	X	X	X

TL, tendon length; FBL, fiber bundle length; X, absent at this level.
*, muscle length = TL + FBL.

intosh and Bogduk, 1986), the force that the muscle can generate depends on many factors including the degree of activation, the muscle volume, as well as the architectural arrangement of the fiber bundles (Lieber and Friden, 2000; Adams, 2002; Kiesel et al., 2007). Each "fascicle" making up LMT consists of not one, but many hundreds of muscle fiber bundles, each with its own unique FBA. In contrast to previous studies, FBA reported in this study takes into consideration both the number and relative distribution of fiber bundles throughout the volume of LMT, explaining the relatively large standard deviations observed for this architectural parameter.

Intermediate LMT may have a role in controlling intersegmental movement imparted by its broad medial muscular attachment to the lateral border of the spinous process and vertically oriented fiber bundles. Of clinical relevance is the finding that intermediate LMT is absent at L5 and may contribute to the higher incidence of spondylolisthesis and disc prolapse at this level.

The placement and gross morphology of tendons within a muscle influences its function (Lundon, 2003). The medially placed, thick, robust tendon of superficial LMT suggests that this region is capable of producing significant torque in a cranial-caudal direction while the intermediate LMT with its laterally placed and relatively thin tendons is likely to produce less torque but in a caudo-cranial direction.

In this study, deep LMT had the shortest FBL, spanning only two levels, and containing the fewest number of fiber bundles (i.e. had the smallest muscle volume) in comparison to superficial and intermediate regions. Based on its architecture, deep LMT is strategically positioned to provide proprioceptive feedback from the lumbar spine. Hence, deep LMT is less likely to restrain inter-segmental movement except at L5 were the volume and length of fiber bundles was the greatest.

It has been reported that the control and stabilization of the lumbar spine is mediated through the interaction and activity of several trunk muscles (Panjabi, 1992a,b), with strong evidence demonstrating LMT's role in augmenting spinal stiffness (Panjabi et al., 1989; Kaigle et al., 1995; Wilke et al., 1995). Despite this evidence, several of the clinical beliefs regarding this muscle have not been substantiated and require further evaluation (MacDonald et al., 2006). The current study lends further evidence to support the clinical belief that different parts or regions within LMT serve distinct functions. Therapeutic exercises designed to restore normal LMT function should aim to optimize activation and control over all of its parts concurrently. Hence, the rehabilitation of LMT should focus on incorporating exercises which help to increase the strength of the muscle as well as controlling intersegmental movement and proprioception.

The results of this study expand the understanding of the morphology and architecture of LMT. In doing so, the study provides the necessary data to noninvasively visualize specific regions of LMT using ultrasound and to guide electrode placement to study muscle activation patterns electromyographi-cally. This will facilitate the evaluation of normal and pathologic function of LMT and allow evaluation of the effectiveness of specific therapeutic intervention strategies.

ACKNOWLEDGMENTS

REFERENCES

Adams MA. 2002. The Biomechanics of Back Pain. Edinburgh; New York: Churchill Livingstone.

Agur AM, Ng-Thow-Hing V, Ball KA, Fiume E, McKee NH. 2003. Documentation and three-dimensional modelling of human soleus muscle architecture. Clin Anat 16:285–293.

Biedermann HJ, DeFoa JL, Forrest WJ. 1991. Muscle fibre directions of iliocostalis and multifidus: Male-female differences. J Anat 179:163–167.

Bogduk N, Macintosh JE, Pearcy MJ. 1992. A universal model of the lumbar back muscles in the upright position. Spine 17:897–913.

Cholewicki J, Panjabi MM, Khachatryan A. 1997. Stabilizing function of trunk flexor-extensor muscles around a neutral spine posture. Spine 22:2207–2212.

De Foa JL, Forrest W, Biedermann HJ. 1989. Muscle fibre direction of longissimus, iliocostalis and multifidus: Landmark-derived reference lines. J Anat 163:243–247.

Donisch EW, Basmajian JV. 1972. Electromyography of deep back muscles in man. Am J Anat 133:25–36.

Hansen L, de Zee M, Rasmussen J, Andersen TB, Wong C, Simonsen EB. 2006. Anatomy and biomechanics of the back muscles in the lumbar spine with reference to biomechanical modeling. Spine 31:1888–1899.

Hides JA, Richardson CA, Jull GA. 1996. Multifidus muscle recovery is not automatic after resolution of acute, first-episode low back pain. Spine 21:2763–2769.

Hides JA, Jull GA, Richardson CA. 2001. Long-term effects of specific stabilizing exercises for first-episode low back pain. Spine 26:E243–E248.

Kaigle AM, Holm SH, Hansson TH. 1995. Experimental instability in the lumbar spine. Spine 20:421–430.

Kiesel KB, Uhl TL, Underwood FB, Rodd DW, Nitz AJ. 2007. Measurement of lumbar multifidus muscle contraction with rehabilitative ultrasound imaging. Man Ther 12:161–166.

Kim SY, Boynton EL, Ravichandiran K, Fung LY, Bleakney R, Agur AM. 2007. Three-dimensional study of the musculotendinous architecture of supraspinatus and its functional correlations. Clin Anat 20:648–655.

Lieber R, Fridén J. 2000. Functional and clinical significance of skeletal muscle architecure. Muscle Nerve 23:1647–1666.

Lundon K. 2003. Orthopedic Rehabilitation Science: Principles for Clinical Management of Nonmineralized Connective Tissue. Boston: Butterworth-Heinemann.

MacDonald DA, Moseley GL, Hodges PW. 2006. The lumbar multifidus: Does the evidence support clinical beliefs? Man Ther 11:254–263.

Macintosh JE, Bogduk N. 1986. The biomechanics of the lumbar multifidus. Clin Biomech 1:205–213.

Macintosh JE, Valencia F, Bogduk N, Munro RR. 1986. The morphology of the human lumbar multifidus. Clin Biomech 1:196–204.

Moseley GL, Hodges PW, Gandevia SC. 2002. Deep and superficial fibers of the lumbar multifidus muscle are differentially active during voluntary arm movements. Spine 27:E29–E36.

Ng-Thow-Hing V. 2001. Anatomically-Based Models for Physical and Geometric Reconstruction of Humans and Other Animals. In: Department of Computer Science. Toronto: University of Toronto.

Panjabi M, Abumi K, Duranceau J, Oxland T. 1989. Spinal stability and intersegmental muscle forces: A biomechanical model. Spine 14:194–200.

Panjabi MM. 1992a. The stabilizing system of the spine. I. Function, dysfunction, adaptation, and enhancement. J Spinal Disord 5:383–389.

Panjabi MM. 1992b. The stabilizing system of the spine. II. Neutral zone and instability hypothesis. J Spinal Disord 5:390–397.

Roy RR, Ishihara A. 1997. Overview: Functional implications of the design of skeletal muscles. Acta Anat (Basel) 159:75–77.

Solomonow M, Zhou BH, Harris M, Lu Y, Baratta RV. 1998. The ligamento-muscular stabilizing system of the spine. Spine 23:2552–2562.

Wilke HJ, Wolf S, Claes LE, Arand M, Wiesend A. 1995. Stability increase of the lumbar spine with different muscle groups: A biomechanical in vitro study. Spine 20:192–198.